# EXCEPTIONAL ELECTRICAL CONDUCTIVITY AND FRACTURE RESISTANCE OF 3D INTERCONNECTED GRAPHENE FOAM/EPOXY COMPOSITES

J. Jia [a*], X. Sun [a], X. Lin [a], X. Shen [a], Y-W Mai [b], J-K Kim[a]

[a]*Department of Mechanical and Aerospace Engineering, The Hong Kong University of Science and Technology, Clear Water Bay, Kowloon, Hong Kong.*
[b]*Centre for Advanced Materials Technology (CAMT), School of Aerospace, Mechanical and Mechatronic Engineering J07, The University of Sydney, Sydney, NSW 2006, Australia*
**To whom correspondence should be addressed: karenjjjia@ust.hk*

**Keywords:** graphene foams, epoxy-matrix composites, electrical conductivity, mechanical properties.

**Abstract**
*Cellular-structured graphene foam (GF)/epoxy composites are prepared based on a three-step fabrication process involving infiltration of epoxy into the porous GF. The 3D interconnected graphene network serves as fast channels for charge carriers, giving rise to a remarkable electrical conductivity of the composite, 3 S/cm, with only 0.2 wt% GF. The corresponding flexural modulus and strength increase by 53% and 38%, respectively, whereas the glass transition temperature increases by a notable 31 ℃, compared to the solid neat epoxy. The GF/epoxy composites with 0.1 wt% GF also deliver an excellent fracture toughness of 1.78 MPa·m$^{1/2}$, 34% and 70% enhancements against their 'porous' epoxy and solid epoxy counterparts, respectively.*

## 1. Introduction

Graphene has attracted tremendous attention owing to its large surface area, high strength and Young's modulus, as well as extraordinary electronic properties and thermal conductivity [1,2]. As a precursor for graphene, graphene oxide (GO) enjoys an abundance of oxygenated functional groups on its surface which offer high processability and dispersibility in aqueous media. These properties make GO an ideal, multi-functional nanofiller to prepare well-dispersed polymer nanocomposites with a tailored nanostructure and interphase. However, there are a number of challenges that need to be addressed to maximize the reinforcement efficiency of graphene. Most importantly, the graphene nanosheets should be fully exfoliated and uniformly dispersed in the polymer to avoid re-agglomeration, especially at high graphene contents, caused by the intermolecular π-π stacking attraction forces [3]. Lack of exfoliation and dispersion of graphene sheets is always detrimental to achieving desired effects on mechanical, electrical, thermal and other important properties. Another critical issue arising from the highly oxygenated GO sheets is that GO sheets ought to be reduced to

recover the $sp^2$ carbon structure to restore the inherently high electrical conductivities of graphene and the composites made therefrom. A newly emerged three dimensional (3D) interconnected graphene foam (GF) by chemical vapor deposited (CVD) has satisfied the above two requirements as nanofillers for polymer composites and gained increasingly interest for application. A typical method to prepare GF/polymer composites is by infiltrating free-standing GF with different kinds of polymers, ultimately eliminating the problems associated with graphene agglomeration in polymers. The electrical conductivity of GF/polydimethyl siloxane (PDMS) foam composite reached 2 S/cm while the compressive strength of GF/epoxy composites showed a notable 55% improvement compared to neat epoxy [4,5]. Composites can also be prepared by infiltrating a prepolymer into the graphene grown on a Ni foam (G-Ni foam), followed by epoxy curing and dissolving the Ni foam template. The resultant GF/epoxy composite prepared in this way contained interconnected micro-scale voids created in place of the Ni template, forming an interconnected cellular structure [6]. Compared to the above solid GF composites, the cellular-structured composites are lighter and possess good liquid permeability; and the porous structure can potentially enhance the fracture toughness of the composites as in the porous polymer thin films [7]. However, the study of this porous composites is still at its infant stage and very few studies have appeared in the open literature reporting their properties.

This paper reports the mechanical properties, fracture toughness and transport properties of the porous GF/epoxy composites. The composites were synthesized by impregnation of epoxy resin into the 3D G-Ni foam via CVD, followed by curing of the polymer and etching of the Ni template.

## 2. Experimental and Characterizations

G-Ni foam was prepared by template-directed CVD process (Figure 1a, b). Both monolayer and few-layer graphene were co-existent in the GF prepared (Figure 1c). Figure 1d shows an approximately linear relationship between $CH_4$ concentration, average number of graphene layers and GF density. The fabrication process for GF/epoxy composites consisted of three steps, as shown in the Figure 2: namely, (i) impregnation of diluted epoxy resin (LY1556, supplied by Huntsman Advanced Materials) into the porous G-Ni foam to produce prepreg; (ii) evaporation of solvent for 5 h in a vacuum oven and curing of epoxy; and (iii) etching of Ni template in HCl (3M at 80 °C /48 h) to create cellular-structured composites. The composites produced thereby contained GF in the range from 0.11 to 0.53 wt%. For comparison of the properties with those of the GF/epoxy composites, the Ni template without graphene layers was impregnated with the same epoxy resin system and cured employing the same procedure as above. The Ni template was etched similarly to produce rectangular plates of neat epoxy containing voids created in place of Ni template, which was designated as 'porous epoxy' with an average pore volume of ~19 vol%.

An optical microscope (Olympus BX51M) and a scanning electron microscope (SEM, JEOL JSM-6700F) with a 5 kV accelerating voltage were used to characterize the morphologies of GF and fracture surface of GF/epoxy composites. The structure of GF was evaluated on a Micro-Raman spectrometer (Renishaw MicroRaman/Photoluminescence System) with Ar laser excitation of 514.5 nm in wavelength. The electrical conductivity was measured based on the four-point probe method using a resistivity/Hall measurement system (Scientific Equipment & Services). To reduce the contact resistance between the probes and the composite surface, the contact points were coated with silver paste. The glass transition temperatures, $T_g$, of the solid epoxy and the GF/epoxy composites were characterized by a

modulated differential scanning calorimeter (DSC, QA1000, TA Instruments). Measurements were conducted at a ramp rate of 10 °C/min in a nitrogen atmosphere. Flexural tests were performed using a universal testing system (Instron 3382) according to the specification, ASTM standard D790-10. The quasi-static mode I fracture toughness, $K_{IC}$, was measured using the single-edge-notch bending (SENB) specimens of 66.0 mm long × 14.0 mm wide × 7.0 mm thick according to the specification, ASTM standard D-5045.

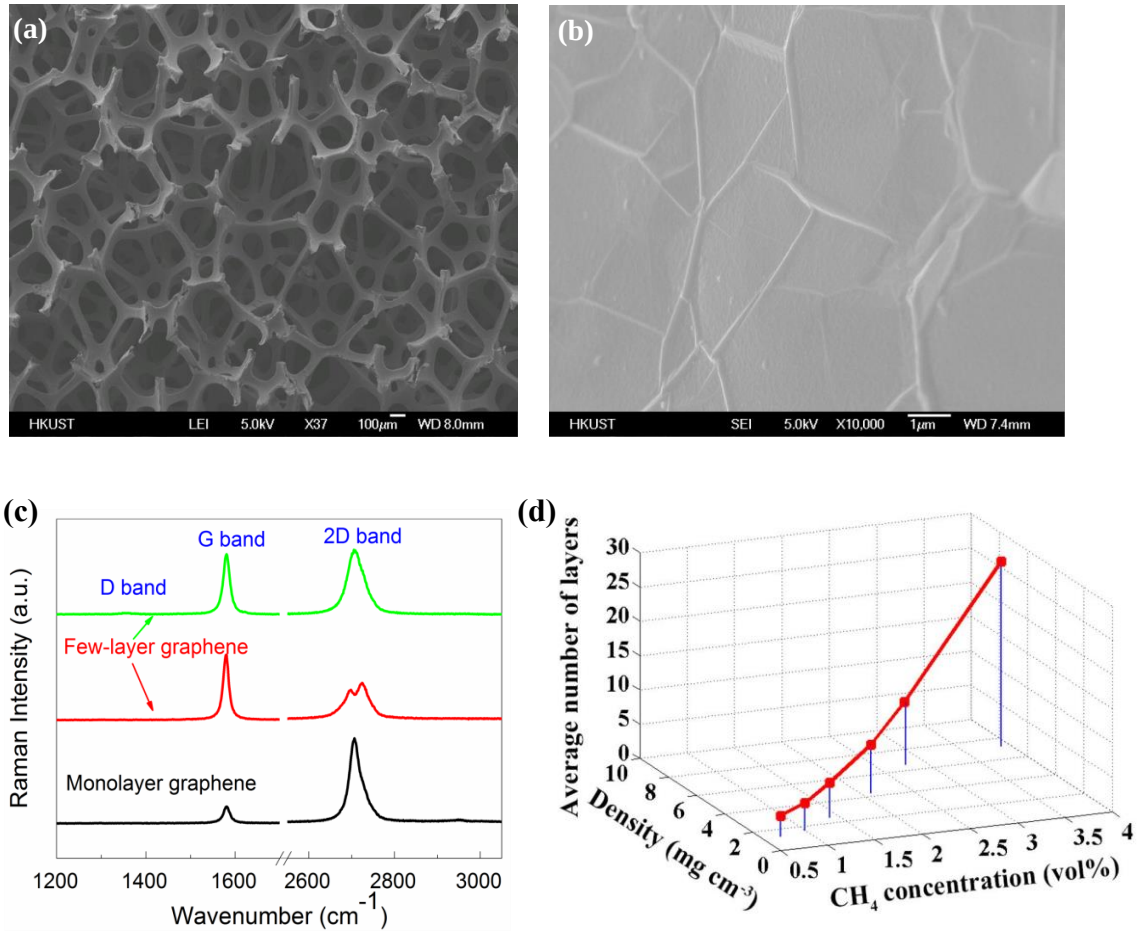


**Figure 1.** (a) SEM image of GF; (b) magnified view of foam surface; (c) Raman spectra of GF prepared; and (d) density and average number of graphene layers of GF as a function of $CH_4$ concentration used in CVD growth.

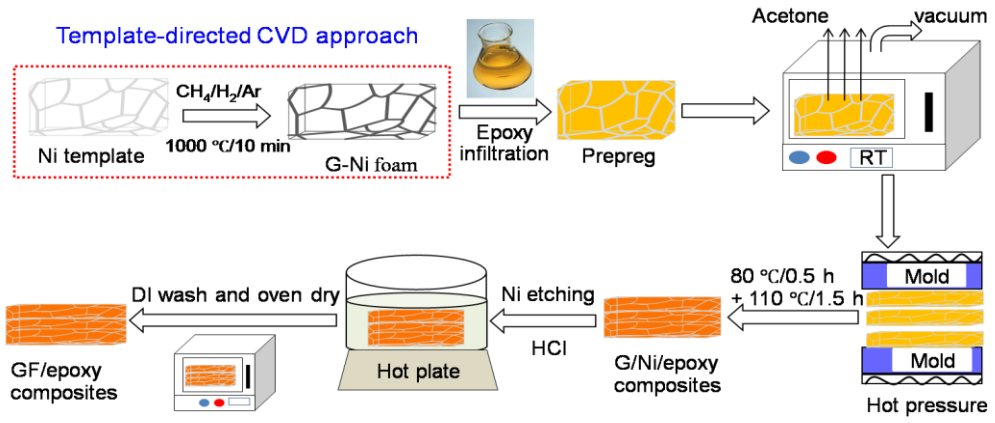


**Figure 2.** Flow chart for the preparation of GF/epoxy composites.

## 3. Results and discussion

### *3.1 Porous structure of GF/epoxy composites.*

Figure 3a shows a typical optical image of a polished cross-section of the GF/epoxy composite containing 0.2 wt% GF. The microcellular pores were present between the nearly spherical blocks of epoxy in the form of curved triangular, dog-bone shapes, resembling the profile of the porous Ni template. These pores with average sizes in the range of tens to hundreds of micrometers were interconnected throughout the composite (Figure 3b,c). The pore volume fraction estimated from the measured densities of the solid epoxy (1.19 g/cm$^3$) and GF/epoxy composites (0.96 g /cm$^3$) was 19.3 vol%. This value is consistent with the average value of 18.7 vol% obtained from the analysis of more than 30 micrographs of polished composite cross-sections. Considering the average thickness of the GF strut is only ~30 nm and assuming that the pressure applied during curing did not distort the Ni template structure, the pore volume in the 'porous epoxy' without GF should be much similar to that in the composite. Figure 3d indicates that the GF adhered well to the epoxy matrix showing excellent resin permeability of the G-Ni foam due to the large surface area and the presence of interconnected pores.

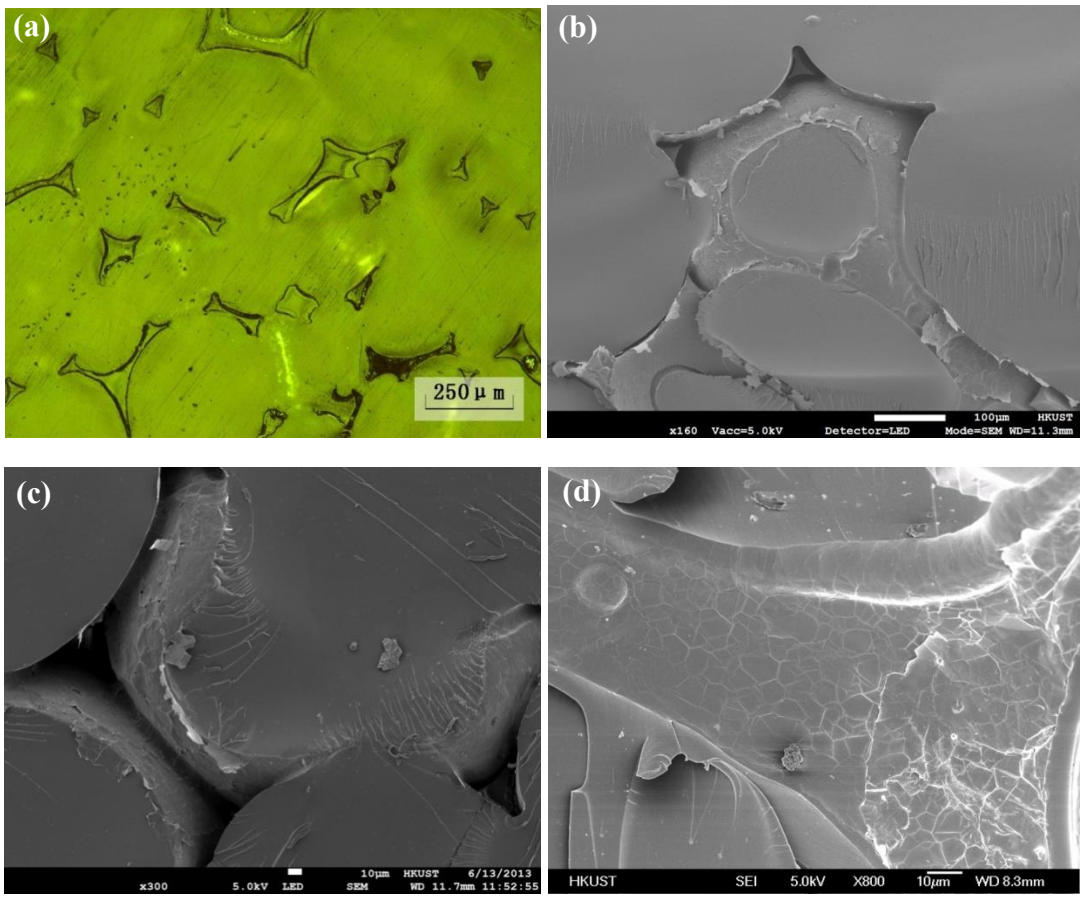


**Figure 3.** (a) Polished surface of a GF/epoxy composite showing pore distribution; (b-d) typical SEM images of GF/epoxy composites containing 0.2 wt% GF prepared at a $CH_4$ concentration of 1.4 vol%.

### *3.2 Glass transition temperature and electrical properties.*

Figure 4a shows that the $T_g$ of the composites increased drastically from 94.9 °C to 126.2 °C with only 0.2 wt% GF content as a result of the hindrance of molecular mobility in the vicinity of GF. Rheological percolation phenomenon or percolated interphase was responsible for the saturation of $T_g$ at higher graphene contents [8]. In view of the random orientation and wrinkled surface of multilayer GF (Figure 1b), it is easy to understand why the percolation at 0.2 wt% GF in this study was higher than the reported 0.05 wt% for FGS/PMMA composites [9]. However, judging from our recent work on aligned rGO/epoxy composites where less than 20 °C increase in $T_g$ was observed at 2.0 wt% rGO [10], GF appears to be much more efficient for improving the thermal stability of epoxy than rGO sheets. At least two important factors contributed to this observation. Firstly, re-agglomeration of graphene in the matrix was spontaneously eliminated by the network structure of GF and the robustness of processing method, resulting in an increased surface area necessary for contacting with the polymer matrix. This naturally created a substantial interphase region around graphene where the mobility of the polymer chains is constrained [11]. Secondly, the nanoscale surface roughness of GF with many ripples likely resulted in enhanced mechanical interlocking with the polymer chains and consequently better interfacial adhesion, both of which had positive effects on thermal stability of the matrix. A similar effect has been suggested by recent molecular dynamics simulation, showing altered polymer chain dynamics because of the geometric constraints at the nanofiller surfaces [12].

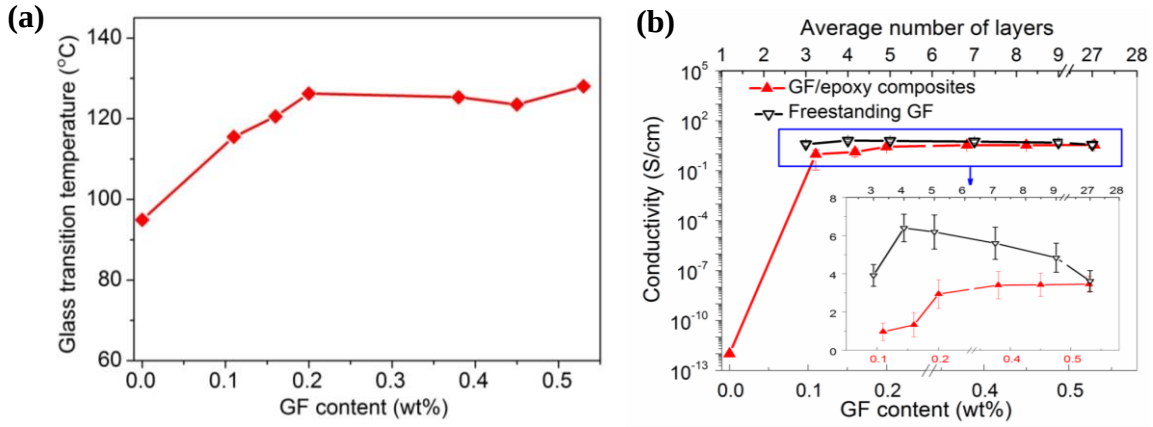


**Figure 4.** (a) Glass transition temperature and (b) electrical conductivity of GF/epoxy composites as a function of GF content. The conductivity of freestanding GF is superimposed in inset of (b).

Figure 4b shows an electrical conductivity of $10^{-12}$ S/cm for the neat epoxy resin which is similar to reported values [13]. With the addition of 0.1 wt% GF, the electrical conductivity surged to 0.97 S/cm by twelve orders of magnitude, with a percolation occurring approximately at 0.05 wt% for the GF/epoxy composites. This conductivity value is at least 5 orders of magnitude higher than those of chemically derived graphene composites at graphene contents above percolation [14,15]. The high electron mobility offered by the seamlessly interconnected 3D network of high-quality GF was responsible for the exceptional electrical conducting performance. The inset in Figure 4b indicates that the electrical conductivity of freestanding GF did not show a monotonic increase with the number of graphene layers, and had a maximum conductivity of 6.4 S/cm with four layers of graphene, or 0.16 wt% GF in the composite. This observation is very similar to previous findings on CVD grown GF and GF/PDMS composites where an optimal average number of graphene layer corresponding to the maximum conductivity was identified to be about five [14]. A further increase in GF content beyond 0.38 wt%, or about seven graphene layers, resulted in a rather saturated conductivity of the GF/epoxy composites. It is also interesting to note that the conductivity of

freestanding GF was consistently higher than the GF/epoxy composites until they gradually converged at higher GF contents, suspecting minor damage to the conducting structure of the GF at low contents during the epoxy infiltration and curing at a high temperature.

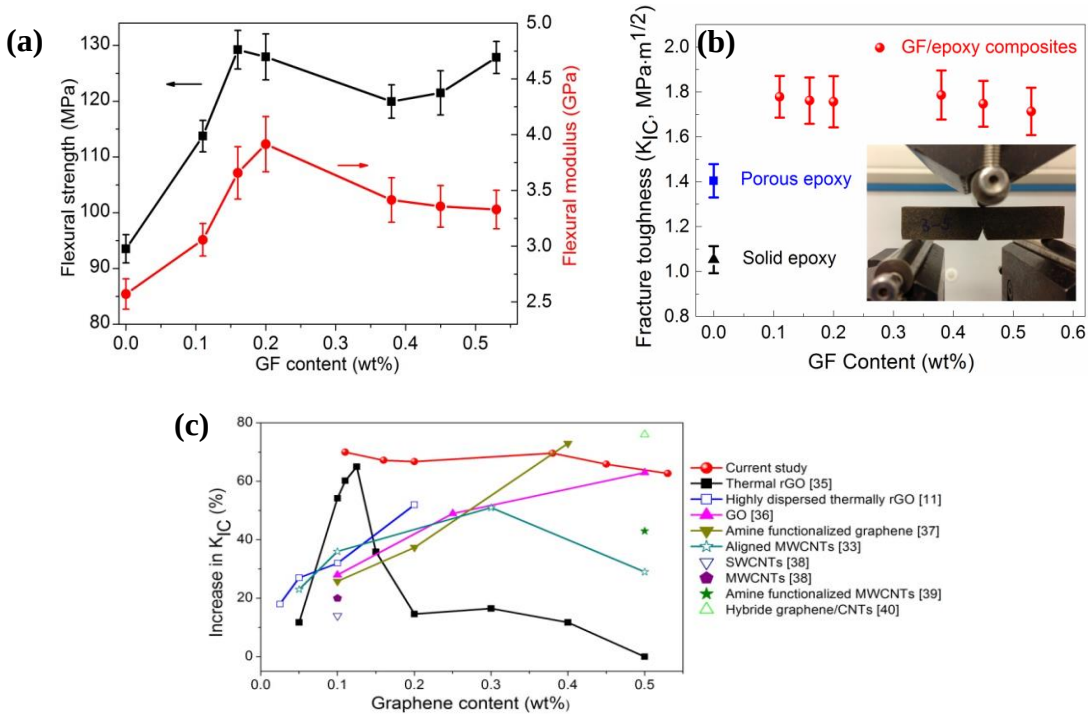


**Figure 5.** (a) Flexural strength and modulus of the solid epoxy and composites as a function of GF content; (b) mode I fracture toughness, $K_{IC}$, plotted as a function of GF content. The inset shows the fracture test of a SENB sample; and (c) comparison of fracture toughness between epoxy-based nanocomposites containing graphene and CNTs taken from literature.

### *3.3 Flexural properties and fracture toughness.*

Incorporation of GF into the epoxy system also significantly increased both the flexural modulus and strength compared to the solid neat epoxy, as shown in Figure 5a. These properties showed maxima at ~0.2 wt% GF with 53% and 38% improvements, respectively, followed by moderate reductions with further increase in GF content – a functionally similar characteristic to $T_g$ (see Figure 4a). This finding signifies the rheological percolation threshold of GF positively affects not only the $T_g$, but also the flexural properties of the GF/epoxy composites. It is well-known that the composite modulus is dependent on the modulus and volume fraction of the composite constituents, whereas the strength is also influenced by the filler-matrix interfacial adhesion [16]. This may explain the relatively moderate improvement of the flexural strength because the GF surface was not specifically functionalized. Figure 5b shows the fracture toughness, $K_{IC}$, of the solid epoxy ~1.05 MPa·m$^{1/2}$, which is consistent with the published values for a similar epoxy system [17]. The $K_{IC}$ value increased sharply to 1.78 MPa·m$^{1/2}$ at 0.1 wt% GF, corresponding to a remarkable enhancement of 70% compared to the solid epoxy. There was an apparent plateau or marginal reductions with further increase in GF content, probably because the increased graphene layers only led to slippage between adjacent layers to disrupt the weak van der Waals forces when the composites were subjected to an external load [3]. Surprisingly, the 'porous epoxy' prepared from the Ni foam/epoxy composites by etching out Ni showed a moderate value $K_{IC}$ = 1.41 MPa·m$^{1/2}$, about 34% higher than that of the solid epoxy, indicating substantial toughening mechanisms offered by the pores created after removing the Ni template.

To identify the benefits of incorporating GF, fracture toughness $K_{IC}$ values of epoxy-based nanocomposites containing graphene sheets and CNTs taken from the literature are compared with the present study in Figure 5c. Due to the large variations in $K_{IC}$ of solid epoxy resins from 0.5 to 1.63 $MPa \cdot m^{1/2}$ [18,19], the increment of fracture toughness of composites compared to their respective control solid epoxy is reported here. Among many CNT/epoxy composites, the best reported enhancement in $K_{IC}$ was 51% at 0.3 wt% of aligned MWCNTs [13]. However, the $K_{IC}$ of SWCNT/epoxy composites was rather disappointing, delivering 14% improvement with 0.1 wt% SWCNT [20]. The performance of the composites containing graphene was impressive especially when the graphene sheets were preferentially aligned. The maximum reported increase in $K_{IC}$ for rGO/epoxy was 65% at 0.125 wt% [17]. However, improvements were largely impaired at rGO contents higher than 0.125 wt% due to the deteriorated filler dispersion. The corresponding performance of GF/epoxy composites was among the best for all graphene contents and was much better than the GO and rGO counterparts.

## 4. Conclusions

The present study reports the growth of a 3D interconnected GF on a porous Ni template via the CVD method. Cellular-structured GF/epoxy composites were fabricated using the 3D GF based on a three-step fabrication process. A remarkable electrical conductivity of 3 S/cm was delivered at 0.2 wt% GF and a low percolation threshold of 0.05 wt% was achieved owing to the 3D integrated GF structure. There was a notable increase of $T_g$ by 31 °C, along with 53% and 38% enhancements in flexural modulus and strength at ~0.2 wt% GF, respectively. These properties were shown saturated at higher GF contents where the rheological percolation phenomenon or percolated interphase occurred. A remarkable 70% enhancement in fracture toughness of the composites compared to the solid epoxy was achieved at 0.1 wt% GF content. In summary, it is challenging to design materials with concurrent improvements in both strength and fracture toughness because they are often mutually exclusive and in most cases one property is sacrificed for the sake of the other [16]. However, we demonstrated in this work that significant improvements in both modulus/strength and fracture toughness were achieved by introducing a small amount of GF into an epoxy matrix. There is a significant analogy between the composites reinforced by 3D GF and 3D textile composites in terms of their capability to suppress crack propagation through the thickness of the composites, especially under delamination and impact modes of loading, due to the 3D nature of interconnected reinforcement structure.

**Acknowledgement.** The project was financially supported by the Research Grants Council of Hong Kong SAR (Project codes: 614010, 613811) and the Australian Research Council (Discovery Project DP130104648).

## References

[1] A. K. Geim and K. S. Novoselov. The Rise of Graphene. Nat. Mater, 6 (3), 183-191, 2007.
[2] C. Lee, X. Wei, J. W. Kysar and J. Hone. Measurement of the Elastic Properties and Intrinsic Strength of Monolayer Graphene. Science, 321 (5887), 385-388, 2008.
[3] L. C. Tang, Y. J. Wan, D. Yan, Y. B. Pei, L. Zhao, Y. B. Li, L. B. Wu, J. X. Jiang, G. and Q. Lai. The Effect of Graphene Dispersion on the Mechanical Properties of Graphene/Epoxy Composites. Carbon, 60, 16-27, 2013.

[4] Z. Chen, C. Xu, C. Ma, W. Ren and H. M. Cheng. Lightweight and Flexible Graphene Foam Composites for High-Performance Electromagnetic Interference Shielding. Adv. Mater, 25 (9), 1296-1300, 2013.
[5] X. Chen, Y. Lu, X. Zhang and F. Zhao. The Thermal and Mechanical Properties of Graphite Foam-Epoxy Resin Composites. Mater. Des, 40, 497-501, 2012.
[6] X. Li, P. Sun, L. Fan, M. Zhu, K. Wang, M. Zhong, J. Wei, D. Wu, Y. Cheng and H. Zhu. Multifunctional Graphene Woven Fabrics. Sci. Rep, 2, 1-8, 2012.
[7] A. V. Kearney, C. S. Litteken, C. E. Mohler, M. E. Mills and R. H. Dauskardt. Pore Size Scaling for Enhanced Fracture Resistance of Nanoporous Polymer Thin Films. Acta Mater, 56 (20), 5946-5953, 2008.
[8] A. K. Kota, B. H. Cipriano, M. K. Duesterberg, A. L. Gershon, D. Powell, S. R. Raghavan and H. A. Bruck. Electrical and Rheological Percolation in Polystyrene/MWCNT Nanocomposites. Macromolecules, 40 (20), 7400-7406, 2007.
[9] T. Ramanathan, A. A. Abdala, S. Stankovich, D. A. Dikin, M. Herrera-Alonso, R. D. Piner, D. H. Adamson, H. C. Schniepp, X. Chen and R. S. Ruoff. Functionalized Graphene Sheets for Polymer Nanocomposites. Nat. Nanotechnol, 3 (6), 327–331, 2008.
[10] N. Yousefi, X. Lin, Q. Zheng, X. Shen, J. R. Pothnis, J. Jia, E. Zussman and J. K. Kim. Simultaneous in Situ Reduction, Self-Alignment and Covalent Bonding in Graphene Oxide/Epoxy Composites. Carbon, 59, 406-417, 2013.
[11] A. Bansal, H. Yang, C. Li, K. Cho, B. C. Benicewicz, S. K. Kumar and L. S. Schadler. Quantitative Equivalence Between Polymer Nanocomposites and Thin Polymer Films. Nat. Mater, 4 (9), 693-698, 2005.
[12] G. D. Smith, D. Bedrov, L. Li and O. Byutner. A Molecular Dynamics Simulation Study of the Viscoelastic Properties of Polymer Nanocomposites. J. Chem. Phys, 117 (20), 9478-9489, 2002.
[13] S. U. Khan, J. R. Pothnis and J. K. Kim. Effects of Carbon Nanotube Alignment on Electrical and Mechanical Properties of Epoxy Nanocomposites. Compos. Part A: Appl. Sci. Manuf, 49, 26-34, 2013.
[14] Z. Chen, W. Ren, L. Gao, B. Liu, S. Pei and H. M. Cheng. Three-Dimensional Flexible and Conductive Interconnected Graphene Networks Grown by Chemical Vapour Deposition. Nat. Mater. 2011, 10, 424-428.
[15] S. Stankovich, D. A. Dikin, G. H. B. Dommett, K. M. Kohlhaas, E. J. Zimney, E. A. Stach, R. D. Piner, S. T. Nguyen and R. S. Ruoff. Graphene-Based Composite Materials. Nature, 442 (7100), 282-286, 2006.
[16] J. K. Kim and Y. W. Mai. Engineered Interfaces in Fiber Reinforced Composites. Elsevier, Oxford, 1998.
[17] M. A. Rafiee, J. Rafiee, I. Srivastava, Z. Wang, H. Song, Z. Z. Yu and N. Koratkar. Fracture and Fatigue in Graphene Nanocomposites. Small, 6 (2), 179-183, 2010.
[18] M. Fang, Z. Zhang, J. Li, H. Zhang, H. Lu and Y. Yang. Constructing Hierarchically Structured Interphases for Strong and Tough Epoxy Nanocomposites by Amine-Rich Graphene Surfaces. J. Mater. Chem, 20 (43), 9635-9643, 2010.
[19] S. Chatterjee, F. Nafezarefi, N. H. Tai, L. Schlagenhauf, F. A. Nüesch and B. T. T. Chu. Size and Synergy Effects of Nanofiller Hybrids Including Graphene Nanoplatelets and Carbon Nanotubes in Mechanical Properties of Epoxy Composites. Carbon, 50 (15), 5380-5386, 2012.
[20] M. A. Rafiee, J. Rafiee, Z. Wang, H. Song, Z. Z. Yu and N. Koratkar. Enhanced Mechanical Properties of Nanocomposites at Low Graphene Content. ACS Nano, 3 (12), 3884-3890, 2009.